

# Simulating boreal forest carbon dynamics after stand-replacing fire disturbance: insights from a global process-based vegetation model

C. Yue<sup>1</sup>, P. Ciais<sup>1</sup>, S. Luysaert<sup>1</sup>, P. Cadule<sup>1</sup>, J.W. Harden<sup>2</sup>, J.T. Randerson<sup>3</sup>, V. Bellassen<sup>4</sup>, T. Wang<sup>1</sup>, S.L. Piao<sup>5</sup>, B. Poulter<sup>1</sup>, N. Viovy<sup>1</sup>

<sup>1</sup>Laboratoire des Sciences du Climat et de l'Environnement, LSCE CEA CNRS UVSQ, 91191 Gif-sur-Yvette, France

<sup>2</sup>US Geological Survey, Menlo Park, CA, USA

<sup>3</sup>Department of Earth System Science, University of California, Irvine, California, USA

<sup>4</sup>CDC Climat, 47 rue de la Victoire, 75009 Paris, France

<sup>5</sup>Department of Ecology, College of Urban and Environmental Science, Peking University, Beijing 100871, China

## Supplementary Material

### 1 Fire combustion fraction for different carbon pools

This section describes how the fuel combustion fractions used in ORCHIDEE-FM-BF are determined by matching the observations in boreal forests. Two types of fuel are available for a typical boreal forest crown fire: ground fuels (or the organic soil layer), which may be comprised of a moss layer, fine litter and an undergrowth of herbaceous plants and small shrubs; and crown fuels, which are mainly the trees' aboveground live biomass and shrubs if present. Regional datasets and experimental fire studies show that fire carbon emissions are dominated by ground fuels (Stocks, 1987, 1989; Amiro et al., 2001; Kasischke and Hoy, 2012). Therefore, most of the fire emissions must be modeled to come from ground fuel burning. As ORCHIDEE-FM-BF does not simulate a profile of litter through the different vertical horizons that occur in the boreal organic soil, the total amount of aboveground litter is considered as the ground fuel.

Previous studies indicate that fuel combustion fractions in fires are not constant and depend on multiple factors (de Groot et al., 2009; Turetsky et al., 2011). However the present study does not seek accurate simulation of combustion fraction and thus simple fixed combustion fractions were adopted for different types of fuel. Kasischke et al. (2000) reported an average combustion fractions of 0.43 (ranging from 0.20 to 0.89) for ground fuels and 0.36 (ranging from 0.22 to 0.48) for live biomass in black spruce fires in the interior of Alaska. We therefore assume combustion fractions of 1.0, 0.9 and 0.3 for metabolic, structural and woody litter respectively. These fractions

correspond to a mass-weighted mean combustion fraction of 0.3 for total ground fuel.

In boreal forest fires, the crown fuel combustion was found to be limited to small branches and needles (Stocks, 1987, 1989; Amiro et al., 2001; Kasischke and Hoy, 2012). In ORCHIDEE-FM-BF, leaf biomass is represented but branches are not accounted for explicitly. Rather, we assume that 90% of the aboveground sapwood and 2% of the heartwood could be considered as small branches and will be burned in fire. These fractions are determined with the relative size of each pool being taken into account.

For aboveground biomass combustion, we set the combustion fractions as 0.9, 0.9, 0.02, 0.7, and 0.7 for leaf, aboveground sapwood and heartwood, fruit and carbon reserve respectively. Since there is no tree survival during the fire, the unburned aboveground heartwood is transferred to the snag pool, and all other unburned biomass parts (with a relatively small size) enter the litter pool (via the litter buffer) immediately after fire. During fires, black carbon could be generated from incomplete burning and this would accumulate in the underlying mineral soil (Kane et al., 2007), but the amount is small and is not explicitly considered in this study.

The parameterization of fire combustion fraction and the fractions of carbon being transferred to litter for various carbon pools are summarized in Fig. S1. Under this scheme, the mass-weighted mean combustion fraction is 7% for aboveground live biomass and 30% for ground litter.

## **2 Climate forcing data**

ORCHIDEE-FM-BF is driven by high frequency (30-minute resolution) data, but can also accommodate low frequency climate forcing data (e.g., monthly resolution). In the case of low frequency data, the model used a weather generator to create the 30-minute climate fields for the model input. In this study, two different sets of climate forcing data are used to drive the model.

First, monthly meteorological fields were retrieved from meteorological stations located close to the evaluation sites. For the Alaska sites, data from the meteorological stations at Delta Junction (1941-2006) and Fairbanks (1930-2006) were used. For the Saskatchewan sites, data from the meteorological station at Prince Albert (1943-2006) were used; and for the Manitoba sites, data from the meteorological station at Thompson (1968-2006) were used.

For monthly climate data, seven meteorological fields (precipitation, number of precipitation days, air relative humidity and temperature at 2 m, air temperature amplitude at 2m, total cloud cover, and 10 m windspeed) were required to drive the model. Monthly temperature, monthly total precipitation and monthly temperature amplitude were available for the Saskatchewan and Manitoba sites, but only monthly temperature and monthly precipitation data were available for the Alaska sites. The other meteorological fields that were required by the model were extracted as monthly values from the CRU3.1 data (Climatic Research Unit, University of East Anglia, [http://badc.nerc.ac.uk/view/badc.nerc.ac.uk\\_\\_ATOM\\_\\_dataent\\_1256223773328276](http://badc.nerc.ac.uk/view/badc.nerc.ac.uk__ATOM__dataent_1256223773328276)) at the grid cell corresponding to the geolocation of each evaluation site. These monthly data are referred to as the composite monthly climate data or CMCD.

Second, in situ meteorological measurements (with 30-minute resolution) from the eddy covariance sites were used. For the Manitoba and Saskatchewan sites, data were retrieved from the La Thuile dataset (<http://www.fluxdata.org>). Data for the Alaska sites were provided by J.T. Randerson. These data were gap-filled by using the corrected daily data from ECMWF ERA-Interim (IERA) 0.7 X 0.7 degree reanalysis (for details, see Wang et al., 2012). These high frequency data are used to drive the model only for the EC observation period. Hereinafter we refer to these data as half-hourly climate data or HHCD.

### **3 Match model outputs with field measurements for woody debris, forest floor and mineral soil carbon**

Due to the difference in the scope of the forest floor and woody debris between field measurement and modeling, in this section we develop a scheme to match the model output with field measurements of these variables.

The terminology, measurement scope and reporting of forest woody detritus in the field are not consistent among different researchers. For example, Bond-Lamberty and Gower (2008) reported total woody detritus as the sum of standing dead wood (SDW, dead wood with zenith angle  $\leq 45^\circ$ ) and downed dead wood (DWD, woody detritus with diameter  $>1$  cm with zenith angle  $> 45^\circ$ ). Whereas Wang et al. (2003) reported them as standing dead tree (STD) and coarse woody debris (CWD). Goulden et al. (2011) reported coarse woody debris to include downed

woody debris with diameters  $\geq 7$  cm (Goulden et al., 2011; Manies et al., 2005). In this study, we adopt the term used by Bond-Lamberty and Gower (2008): total woody debris (TWD) consists of standing dead wood (STD, with zenith angle  $\leq 45^\circ$  in field measurements), and downed woody debris (DWD, snags with zenith angle  $>45^\circ$  and woody detritus lying on the ground).

Furthermore, in field measurements the heavily decomposed fine woody debris is always sampled as part of the forest floor or organic soil (Wang et al., 2003; Goulden et al., 2011). Thus, for the aboveground part, the sum of aboveground litter and snags in the model should be equal to the sum of forest floor and total woody debris in field measurements (Fig. S2). As shown in Fig. S2, to compare modeled DWD with measurement, 30% of the aboveground snag in the model was treated as DWD. This fraction was determined to make the ratio of DWD to TWD equal to the chronosequence average ratio reported by Bond-Lamberty and Gower (2008). The remaining 70% of modeled snag carbon is compared with the standing dead wood in the field measurement.

To compare the modeled forest floor carbon with measurement, 75% of aboveground woody litter in the model was counted as forest floor (Fig. S2). This fraction was selected to optimize the model-measurement comparison for forest floor carbon and DWD simultaneously. The remaining 25% of modeled woody litter is counted as DWD.

Finally, the mineral soil carbon in the model is added together with belowground litter to be compared with measured mineral soil carbon. The model-data matching is summarized in Fig. S2, which allows closure of all carbon stock compartments between model and measurement.

#### **4 Model improvement in ORCHIDEE-FM-BF compared to the standard version**

Fig. S3 shows the simulated GPP, NEP, heterotrophic respiration and total biomass carbon for the 19<sup>th</sup> and 20<sup>th</sup> fire rotations and the postfire simulation by ORC-STD, ORC-FM-NOSNAG and GPPCAL-CMCD simulations, for the sites in Manitoba.

Moving from standard ORCHIDEE to ORCHIDEE-FM (or ORCHIDEE-FM-BF) significantly improved simulation results. Simulated GPP, total biomass carbon and heterotrophic respiration by ORC-STD are all higher (1~2 times) than the measurement. As all the unburned biomass enters into the litter pool immediately after fire, the heterotrophic respiration simulated by ORC-STD surges to an unrealistically high level of  $6000 \text{ g C m}^{-2} \text{ yr}^{-1}$ , rendering the ecosystem an

extremely big carbon source of  $6000 \text{ g C m}^{-2} \text{ yr}^{-1}$  (compared with measured NEP of  $-150 \text{ g C m}^{-2} \text{ yr}^{-1}$  by Goulden et al., 2011 and  $-202 \pm 53 \text{ g C m}^{-2} \text{ yr}^{-1}$  by Randerson et al. 2006). In contrast, the results from the ORC-FM-NONSAG and GPPCAL-CMCD simulations agree more closely with the measurements.

There is no difference in simulated GPP and total biomass carbon between the ORC-FM-NOSNAG and GPPCAL-CMCD simulations. Within ~20 years after fire, simulated heterotrophic respiration by ORC-FM-NOSNAG is slightly higher than GPPCAL-CMCD; this is expected because all the unburned biomass turns into litter immediately after fire in the ORC-FM-NOSNAG simulation where it contributes to heterotrophic respiration.

It is slightly surprising that adding the snag process does not lead to significant improvement in model-measurement agreement in terms of postfire NEP trajectory shortly after fire (inset plot in Fig. S3b). This reflects the complexity of modeling, and may indicate that other processes are still missing from the model; including for example, the respiration of snags. Besides, the model assumed a first order kinetic function with time to simulate snag falling and mixing with litter, while in reality the timing of snags entering decomposition is highly variable. Hilger et al. (2012) further demonstrated that the mass transfer rate between snags and litter differed from the snag falling rate, which was derived by tree number counting.

A detailed and more accurate simulation of the snag-related heterotrophic process requires more measurement data that should include both the postfire snag and litter amount as well as all the components of carbon fluxes (GPP, NPP and heterotrophic respiration, with a distinction made between soil and litter components). Such an analysis is beyond the scope of the study presented here. Nevertheless, the inclusion of the snag pool in the model allowed the direct comparison of this carbon stock with measurement, and allows the model to represent one of the important long-term after-fire carbon stocks (Manies et al., 2005).

## **5 Evaluation of mineral soil organic carbon**

The simulated mineral soil organic carbon begins to increase at the start of the simulation, and is still increasing slowly ( $\sim 0.002 \text{ kgCm}^{-2}\text{yr}^{-1}$ ) when the simulation reaches the postfire simulation after the most recent fire event. Fig. S4 shows the mean simulated mineral soil carbon

over the postfire period, averaged over all sites, in comparison to the measured data. Our aim is to compare the simulated mineral soil carbon with the observed data in a qualitative way rather than to examine the postfire temporal evolution (as opposed to the comparison for other variables in the main texts). For this reason, the metrics in Sect. 2.5 in the main text used for quantitative model-measurement comparison with a focus on postfire temporal evolution are not applicable.

The measured mineral soil carbon stocks in Fig. S4 are for the depths of 20-80 cm but are the mean values of several soil profiles. In ORCHIDEE-FM-BF the soil depth is set as 200 cm, and soil carbon is not simulated with explicit empirical depth-dependent turnover rates but with three conceptual pools (fast, slow and passive). So to compare the simulated soil carbon at exactly the measured depth, a root profile or an empirical mineral soil carbon distribution profile is needed to scale this total amount of soil carbon to the measured depths. However, considering the arbitrary soil depth setting in the model, there is risk that this depth scaling could be wrong. Therefore, rather than doing a complete accurate mineral soil carbon model calibration, we focus on the influence of the error in carbon flux estimation that's due to the error in the simulated mineral soil carbon pool and whether this error is acceptable considering other error sources (e.g., the carbon flux measurement error).

The simulated mineral soil carbon agrees best with the well-drained measurements, and is generally smaller than the poorly drained measurements. For Saskatchewan, the simulated mineral soil carbon is ~2 times that at the measured well-drained sites, while in Alaska, the simulated mineral soil carbon stock is half that of the well-drained sites. Therefore, ORCHIDEE-FM-BF only has a moderate-to-low capability of reproducing soil carbon, as it does not fully include decomposition processes (for example, the permafrost influence and cold historical temperature) that affect boreal soils. This variable can either be under- or overestimated by a factor of two across sites, although the spatial heterogeneity of mineral soil carbon in boreal forests is also great due to factors including soil drainage, nutrient availability, soil freezing and vegetation type (Gower et al., 1997).

As ORCHIDEE-FM-BF uses a three-pool model with different turnover rates to simulate mineral soil carbon, the discrepancy in mineral soil carbon between model simulation and measurement makes only a rather small contribution to the simulated carbon fluxes, as the discrepancy in carbon stocks mainly arises from the soil carbon pool with a low turnover rate.

ORCHIDEE-FM-BF includes the effect of soil texture on mineral soil carbon decomposition, and soils with coarser texture (high sand and low clay content) have a faster decomposition rate and thus a lower soil carbon stock. Of the simulation sites in Manitoba (CA-NS1 to CA-NS7), the site CA-NS1 is clay-rich (sand:silt:clay = 0.02:0.13:0.86) and CA-NS7 is sand-rich (sand:silt:clay = 0.27:0.31:0.42). The simulated mineral soil carbon stock is 12.6 kg C m<sup>-2</sup> for CA-NS1 and 4.7 kg C m<sup>-2</sup> for CA-NS7. The difference mainly resides in the pool of mineral soil carbon with slow turnover (see Sect. 2.2 for model description), and this difference results in a 16% difference in heterotrophic respiration (data not shown).

## **6 Evaluation of modeled stand structure**

One particularly interesting feature of ORCHIDEE-FM-BF is that the model equations represent the forest self-thinning process explicitly by comparing on yearly basis the theoretical maximum tree density (through quadratic mean diameter - maximum individual density curve) with modeled tree density. The default parameters for the self-thinning curve for European forests are used in this study (Bellassen et al., 2010); the model predicts the tree density to within 20% of that predicted by a relationship that was derived using local observations (Newton, 2006).

The initial density for all study sites is set as 12,500 trees ha<sup>-1</sup> for the young saplings after fire according to Wang et al. (2003). Simulated stand density, stand basal area (BA) and mean diameter at breast height (DBH) are compared with measurements in Fig. S5. Simulated stand density is found to agree best with observations at the Manitoba dry sites (Fig. S5a). For the young forest (<40 yrs) at wet sites and at the Alaska sites, stand density is overestimated by the model. The overlap ratio between modeled and measured data was 0.27, with the RMSD dominated by unbiased RMSD. For BA and DBH, none of the RTO regression slopes are significantly different from 1, indicating a good model-measurement agreement. The model-measurement overlap ratios are 0.50, 0.33 for DBH and BA respectively.

Supplementary figures and tables

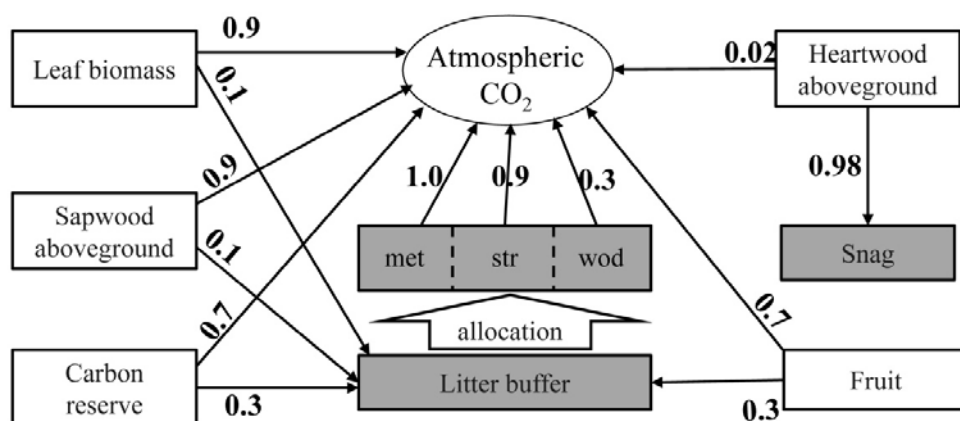


Fig. S1 Fire combustion fractions for various carbon pools, and transfer of unburned live biomass to litter and snag. Numbers in the figure refer to fractions transferred between different pools. Blank rectangles indicate biomass carbon pools and shaded rectangles indicate snag and litter pools. For the three types of litter: met, str and wod refer to metabolic, structural and woody litter, respectively.

Model term	Measurement term	Measurement definition	
Aboveground snag (70%)	Standing dead wood (STD)	Standing dead wood with zenith angle $\leq 45$	Total woody debris (TWD)
Aboveground snag (30%)	Downed woody debris (DWD)	Dead wood debris with zenith angle $> 45$ and woody detritus on ground	
Woody litter (25%)			
Woody litter (75%)	Forest floor	Litter, dead moss and fine woody detritus, which can include few horizons of D/F/M/H	← ground
Structural litter			
Metabolic litter			
Belowground litter	Mineral soil carbon	3 layers if all present: A/B/C	
Active/slow/passive soil carbon			

Fig. S2 The scheme for matching model output with field measurements for woody debris, forest floor and mineral soil carbon

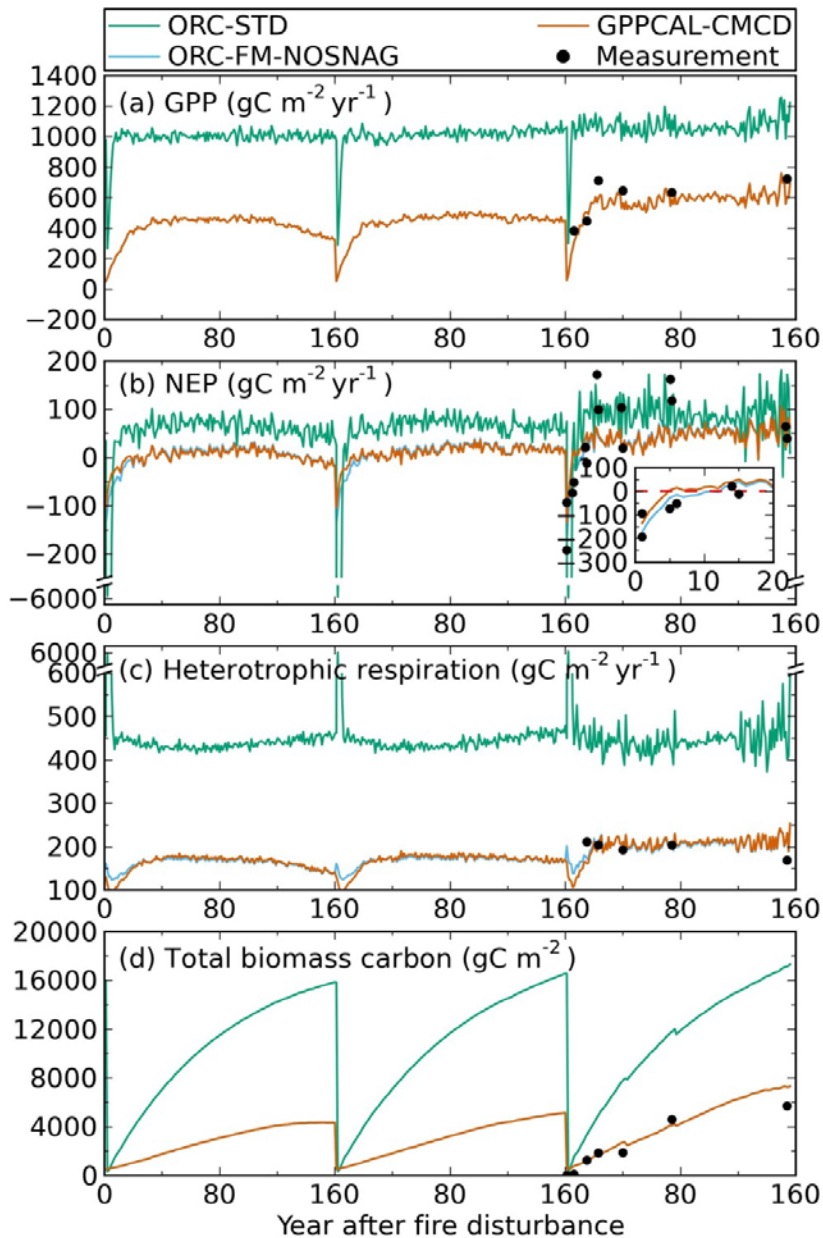


Fig. S3 Simulated (a) GPP, (b) NEP, (c) heterotrophic respiration and (d) total biomass carbon for ORC-STD (bluish green), ORC-FM-NOSNAG (sky blue) and GPPCAL-CMCD (orange) simulations, for Manitoba sites. The results are presented for the mean of the seven evaluation sites (CA-NS1 to CA-NS7). The 19th and 20th fire rotations in the second spinup and the postfire simulation after the most recent fire event are shown, with each step drop of the biomass carbon in subplot (d) indicating a fire event. The inset plot within subplot (b) shows more details of NEP trajectory for 20 years after the most recent fire events for ORC-FM-NOSNAG and GPPCAL-CMCD simulations. In subplots (a) and (d), blue and red lines overlap with each other.

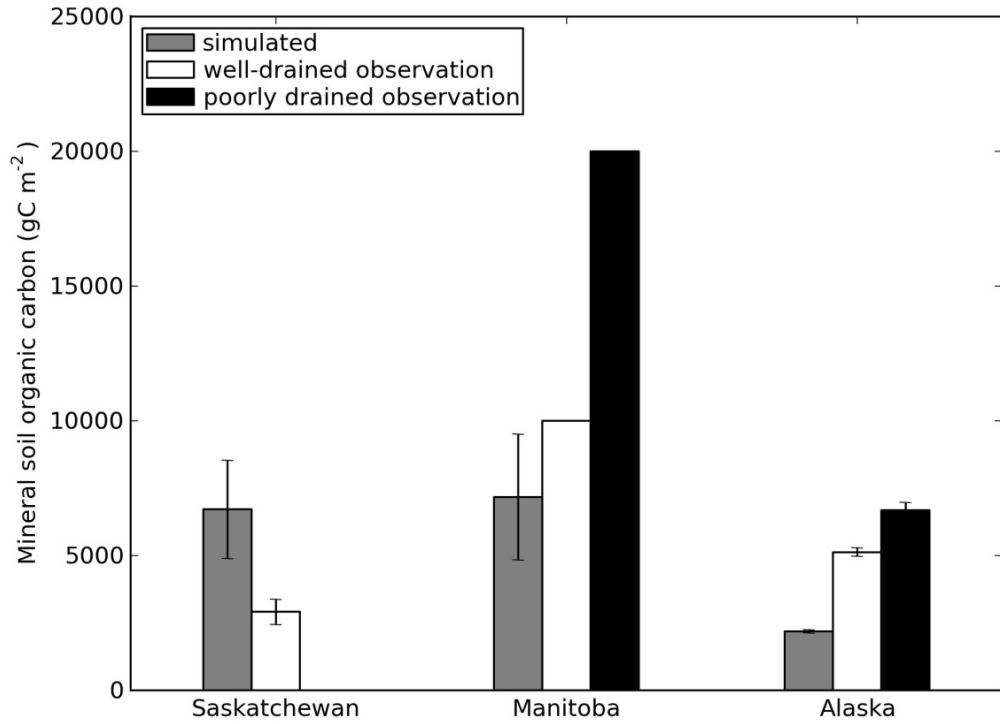


Fig. S4 Comparison of simulated (gray bar) and measured mineral soil carbon (white bar for well-drained observation, black bar for poorly drained observation). Error bars indicate standard deviation among evaluation sites in the same cluster.

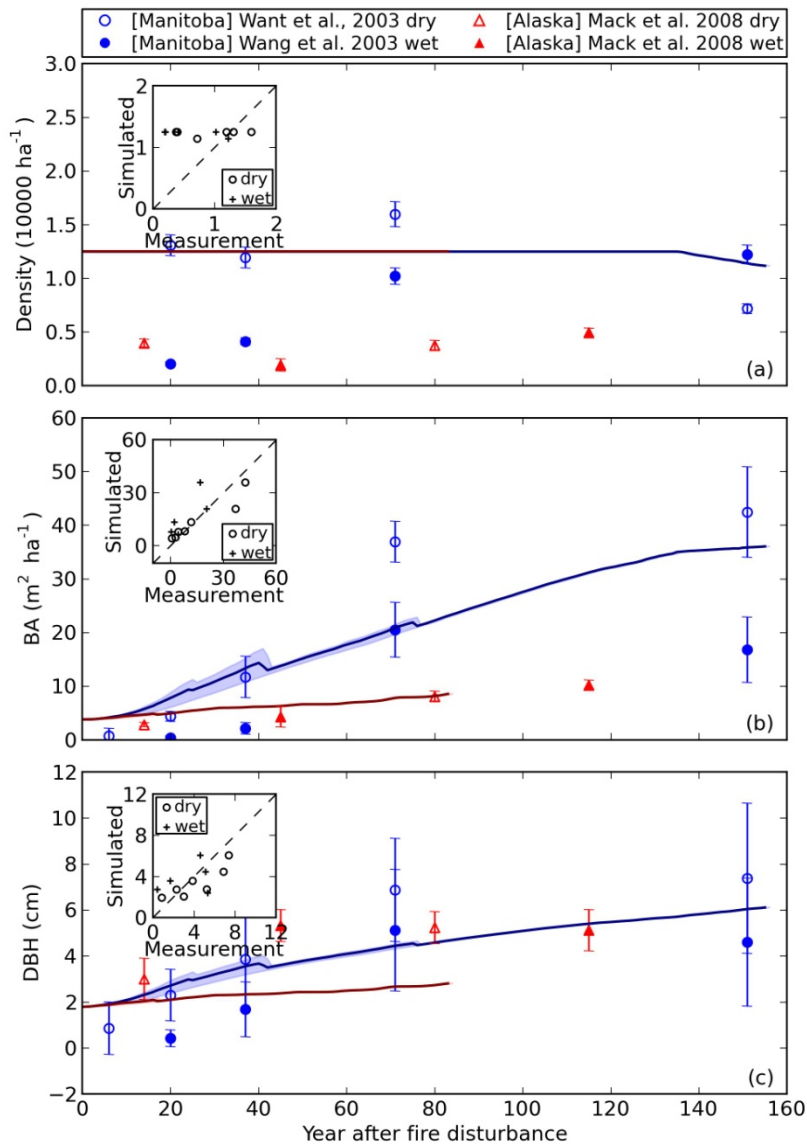


Fig. S5 Simulated versus measured forest (a) individual density, (b) basal area (BA), and (c) mean diameter at breast height (DBH) as a function of time after fire. Observations were only available for Manitoba and Alaska. Model results (Manitoba: blue, Alaska: red) are presented by pooling together outputs for all evaluation sites of the same site cluster, with the solid line indicating the mean value, and shaded area showing between-site minimum-maximum range. Measurements from different sources are shown separately for Manitoba (circles) and Alaska (triangles), with wet (dry) site measurements as filled (open) sign. Error bars on the measurement points indicate 90% confidence interval measurement uncertainty. The inset panel shows the overall model-measurement agreement along a 1:1 ratio line for dry (small open circles) and wet (small cross symbol, "+") measurements separately.

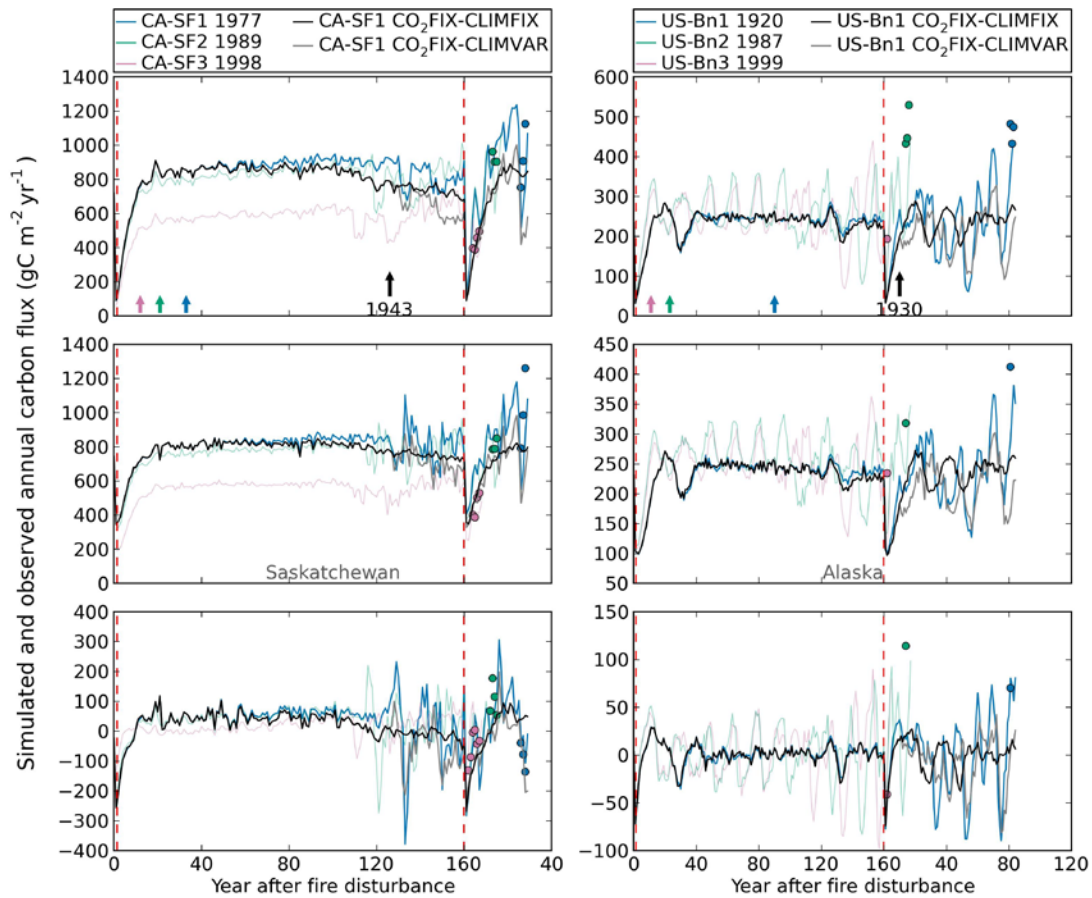


Fig. S6 Simulated GPP (a), TER (b) and NEP (c) trajectory for the time of the 20th fire rotation (since the first red dashed line) and for the chronosequence period (since the second red dashed line). Simulation results for the scenario of varying  $\text{CO}_2$  with varying climate (GPPCAL-CMCD, colored lines) are shown for all evaluation sites in Saskatchewan (CA-SF1 to CA-SF3, left column) and Alaska (US-Bn1 to US-Bn3, right column). Simulation results for the scenarios of fixed  $\text{CO}_2$  with varying climate ( $\text{CO}_2\text{FIX-CLIMVAR}$ , gray lines), and fixed  $\text{CO}_2$  with fixed climate ( $\text{CO}_2\text{FIX-CLIMFIX}$ , black lines) are shown for the sites CA-SF1 and US-Bn1. Corresponding eddy-covariance  $\text{CO}_2$  flux measurements (Amiro et al., 2010; Goulden et al., 2011) at each site are shown as colored dots, with the colors corresponding to the colors of GPPCAL-simulation results for each site. For GPPCAL-CMCD simulation results, the numbers after the site names in the legend indicate the year of most recent fire event. The colored small arrows at the bottom of the first row of panels indicate the time at which atmospheric  $\text{CO}_2$  begins to increase for each site in the GPPCAL-CMCD simulation. The small black arrows with the numbers indicate the year on each site cluster when the meteorological station observed climate data were available.

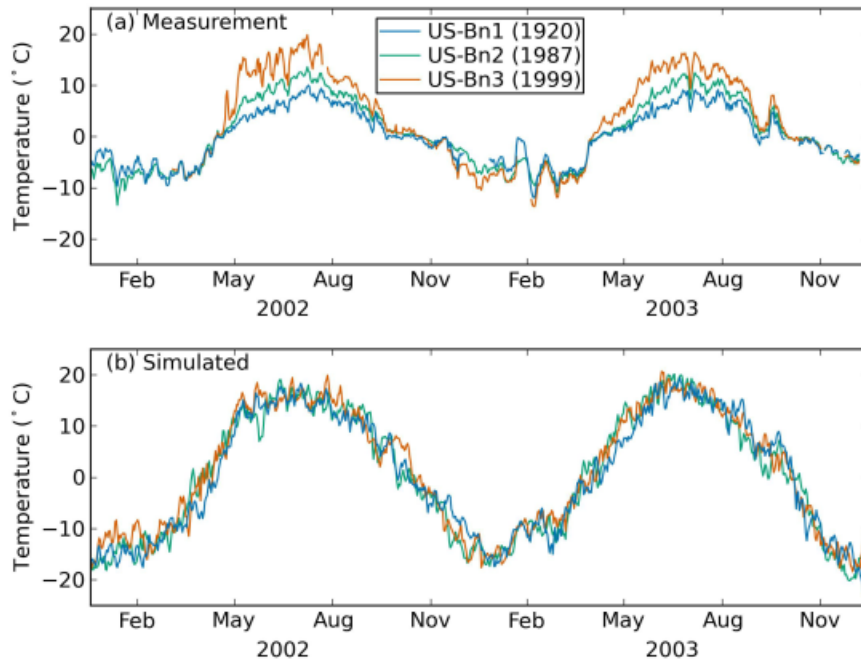


Fig S7 (a) Measured and (b) simulated daily soil temperature for the 0-20 cm soil depth for the year of 2002-2003 at the three Alaskan simulation sites. Measurement data are provided by J.T. Randerson. The numbers within the brackets denote the year of burning for each site.

Table S1 Variables used for validation and their data sources

Variable	Site	Evaluation data source
GPP, NEP, TER	Alaska	Amiro et al., 2010
	Manitoba	
	Saskatchewan	
Leaf Area Index	Manitoba	Goulden et al., 2011; Wang et al., 2003; Bond-Lamberty & Gower, 2008
	Saskatchewan	
	Alaska	
Total biomass carbon	Manitoba	Wang et al., 2003; Goulden et al., 2011
Aboveground biomass carbon	Saskatchewan	Mkabela et al., 2009; Gower et al., 1999
	Alaska	
Woody debris carbon <sup>a</sup>	Manitoba	Bond-Lamberty & Gower, 2008; Wang et al., 2003; Mkabela et al., 2009
Forest floor carbon <sup>b</sup>	Manitoba	Wang et al., 2003; Goulden et al., 2011; Harden et al., 2012
	Saskatchewan	
	Alaska	
Mineral soil carbon <sup>c</sup>	Alaska	Yi et al., 2010; Harden et al., 2012
	Saskatchewan	
	Manitoba	
DBH, Individual density, and Basal Area	Manitoba	Wang et al., 2003
	Alaska	

a. Detailed definitions for woody debris carbon are provided in Sect. 3.

b. Forest floor carbon includes litter, dead moss and fine woody detritus, in distinctive horizons depending on site conditions (Manies et al., 2004, 2006; Manies and Harden, 2011): L (Live moss, dead leaves, twigs, lichen, etc.), D (Dead moss), F (Fibric or fibrous organic layers), M (Mesic organic layers) and H (Humic or sapric organic layers).

c. Mineral soil carbon measurements include three soil layers where present (Manies et al., 2006), A: soil that forms at the surface or below organic horizons with less than 20 percent organic matter; B: mineral soil that has formed below an A horizon with little or none of its original rock structure; C: mineral soil that has been little affected by pedogenic processes.

Table S2 Detailed information for the use of composite monthly climate data in the climate forcing history

Site Name	Period of meteorological station data availability	Climate forcing history			
		First spinup and the first 19 fire rotations of the second spinup <sup>a</sup>	20 <sup>th</sup> fire rotation of the second spinup	Postfire simulation before the EC observation period	Simulation for EC observation period
CA-SF1		1943-76(avg)	1943-76(avg) + 1943-76	1977-2002	2003-2005
CA-SF2	1943-2006	1943-88(avg)	1943-88(avg) + 1943-88	1989-2002	2003-2005
CA-SF3		1943-97(avg)	1943-98(avg) + 1943-98	1998-2002	2003-2005
CA-NS1		1968-80(avg)	1968-80(avg)	1968-80(avg) + 1968-2001	2002-2005
CA-NS2		1968-80(avg)	1968-80(avg)	1968-80(avg) + 1968-2000	2001-2005
CA-NS3		1968-80(avg)	1968-80(avg)	1968-80(avg) + 1968-2000	2001-2005
CA-NS4	1968-2006	1968-80(avg)	1968-80(avg)	1968-80(avg) + 1968-2001	2002-2004
CA-NS5		1968-80(avg)	1968-80(avg)	1981-2000	2001-2005
CA-NS6		1968-88(avg)	1968-88(avg) + 1968-88	1989-2000	2001-2005
CA-NS7		1968-97(avg)	1968-98(avg) + 1968-98	1998-2001	2002-2005
US-Bn1		1930-59(avg)	1930-59(avg)	1930-59(avg) + 1930-2002	2003
US-Bn2	1930-2006	1930-86(avg)	1930-86(avg) + 1943-86	1987-2002	2003
US-Bn3		1930-98(avg)	1943-98(avg) + 1930-98	1999-2002	2003

a. "avg" means the averaged monthly climate forcing data over the specified period.

Table S3 Carbon stock change and accumulated carbon fluxes for simulation of CO<sub>2</sub>FIX-CLIMFIX for the 19th and 20th "fire rotation" of the second spinup and the period after the most recent fire event. Fire carbon emission means the carbon emission for the fire at the beginning of each fire rotation. Mineral SOC: Mineral soil organic carbon stock. NEP-EMI-Cgrowth: NEP minus fire carbon emissions minus growth in the total carbon stocks, the small values in this column indicate that the carbon budget is closed in the model, the big values at site CA-SF1 for the period after most recent fire event is because the model uses yearly output timestep and the error of carbon stocks within the same year.

	<b>FRI</b>	<b>Aboveground litter (g C m<sup>-2</sup>)</b>	<b>Belowground litter (g C m<sup>-2</sup>)</b>	<b>Mineral SOC (g C m<sup>-2</sup>)</b>	<b>Total biomass carbon (g C m<sup>-2</sup>)</b>	<b>Carbon pool increase (g C m<sup>-2</sup>)</b>	<b>Fire carbon emission (g C m<sup>-2</sup>)</b>	<b>Accumulated NEP (g C m<sup>-2</sup>)</b>	<b>NEP-EMI-Cgrowth (g C m<sup>-2</sup>)</b>	<b>Accumulated GPP (g C m<sup>-2</sup>)</b>	<b>Accumulated TER (g C m<sup>-2</sup>)</b>	<b>Emission per year (g C m<sup>-2</sup> yr<sup>-1</sup>)</b>	<b>NEP per year (g C m<sup>-2</sup> yr<sup>-1</sup>)</b>	<b>Period length (yr)</b>
CA-NS1	<b>19th</b>	7	4	147	4	162	963	1123	-2	74013	72890	6	7	160
	<b>20th</b>	-17	-4	90	-155	-86	966	879	-1	73435	72556	6	5	160
	<b>Postfire</b>	5	2	147	41	195	936	1149	18	71525	70376	6	7	155
CA-SF1	<b>19</b>	28	6	64	31	129	3697	3844	18	127913	124069	23	24	160
	<b>20</b>	-109	-12	98	-65	-88	3774	3689	2	127860	124172	24	23	160
	<b>Postfire</b>	1180	770	-29	-6561	-4640	3683	232	1189	19068	18836	23	8	28
US-Bn1	<b>19</b>	7	5	29	14	54	486	541	1	37012	36472	3	3	160
	<b>20</b>	6	2	39	14	60	495	556	0	37433	36878	3	3	160
	<b>Postfire</b>	195	75	65	-361	-26	492	463	-3	19149	18686	3	6	83

Table S4 Carbon stock change and accumulated carbon fluxes for simulation of CO<sub>2</sub>FIX-CLIMVAR for the 19th and 20th "fire rotation" of the second spinup and the period after the most recent fire event. Fire carbon emission means the carbon emission for the fire at the beginning of each fire rotation. Mineral SOC: Mineral soil organic carbon stock. NEP-EMI-Cgrowth: NEP minus fire carbon emissions minus growth in the total carbon stocks, the small values in this column indicate that the carbon budget is closed in the model, the big values at site CA-SF1 for the period after most recent fire event is because the model uses yearly output timestep and the error of carbon stocks within the same year.

	<b>FRI</b>	<b>Aboveground litter (g C m<sup>-2</sup>)</b>	<b>Belowground litter (g C m<sup>-2</sup>)</b>	<b>Mineral SOC (g C m<sup>-2</sup>)</b>	<b>Total biomass carbon (g C m<sup>-2</sup>)</b>	<b>Carbon pool increase (g C m<sup>-2</sup>)</b>	<b>Fire carbon emission (g C m<sup>-2</sup>)</b>	<b>Accumulated NEP (g C m<sup>-2</sup>)</b>	<b>NEP-EMI-Cgrowth (g C m<sup>-2</sup>)</b>	<b>Accumulated GPP (g C m<sup>-2</sup>)</b>	<b>Accumulated TER (g C m<sup>-2</sup>)</b>	<b>Emission per year (g C m<sup>-2</sup> yr<sup>-1</sup>)</b>	<b>NEP per year (g C m<sup>-2</sup> yr<sup>-1</sup>)</b>	<b>Period length (yr)</b>
CA-NS1	<b>19th</b>	7	4	147	4	162	963	1123	-2	74013	72890	6	7	160
	<b>20th</b>	-17	-4	90	-155	-86	966	879	-1	73435	72556	6	5	160
	<b>Postfire</b>	-21	-30	-27	-288	-366	936	600	30	70078	69478	6	4	155
CA-SF1	<b>19</b>	28	6	64	31	129	3697	3844	18	127913	124069	23	24	160
	<b>20</b>	-1186	-80	208	-521	-1579	3774	2169	-27	124985	122817	24	14	160
	<b>Postfire</b>	1291	817	14	-6853	-4731	3047	-408	1276	18065	18473	19	-15	28
US-Bn1	<b>19</b>	7	5	29	14	54	486	541	1	37012	36472	3	3	160
	<b>20</b>	6	2	39	14	60	495	556	0	37433	36878	3	3	160
	<b>Postfire</b>	105	-50	-96	-602	-643	492	-164	-12	16509	16673	3	-2	83

Table S5 Carbon stock change and accumulated carbon fluxes for simulation of GPPCAL-CMCD for the 19th and 20th "fire rotation" of the second spinup and the period after the most recent fire event. Fire carbon emission means the carbon emission for the fire at the beginning of each fire rotation. Mineral SOC: Mineral soil organic carbon stock. NEP-EMI-Cgrowth: NEP minus fire carbon emissions minus growth in the total carbon stocks, the small values in this column indicate that the carbon budget is closed in the model, the big values at site CA-SF1 for the period after most recent fire event is because the model uses yearly output timestep and the error of carbon stocks within the same year.

	<b>FRI</b>	<b>Aboveground litter (g C m<sup>-2</sup>)</b>	<b>Belowground litter (g C m<sup>-2</sup>)</b>	<b>Mineral SOC (g C m<sup>-2</sup>)</b>	<b>Total biomass carbon (g C m<sup>-2</sup>)</b>	<b>Carbon pool increase (g C m<sup>-2</sup>)</b>	<b>Fire carbon emission (g C m<sup>-2</sup>)</b>	<b>Accumulated NEP (g C m<sup>-2</sup>)</b>	<b>NEP-EMI-Cgrowth (g C m<sup>-2</sup>)</b>	<b>Accumulated GPP (g C m<sup>-2</sup>)</b>	<b>Accumulated TER (g C m<sup>-2</sup>)</b>	<b>Emission per year (g C m<sup>-2</sup> yr<sup>-1</sup>)</b>	<b>NEP per year (g C m<sup>-2</sup> yr<sup>-1</sup>)</b>	<b>Period length (yr)</b>
CA-NS1	<b>19th</b>	7	4	147	4	162	963	1124	-1	74013	72890	6	7	160
	<b>20th</b>	-17	-4	90	-155	-86	966	880	0	73435	72556	6	5	160
	<b>Postfire</b>	1132	215	953	2097	4398	936	5324	-10	84248	78928	6	34	155
CA-SF1	<b>19</b>	28	6	64	31	129	3697	3847	20	127913	124069	23	24	160
	<b>20</b>	694	295	650	517	2156	3774	6028	98	134482	128459	24	38	160
	<b>Postfire</b>	951	850	144	-6166	-4222	4097	1107	1232	23714	22607	26	40	28
US-Bn1	<b>19</b>	7	5	29	14	54	486	541	1	37012	36472	3	3	160
	<b>20</b>	25	14	56	72	167	495	662	0	37972	37310	3	4	160
	<b>Postfire</b>	245	6	-40	-273	-63	516	416	-37	19423	19007	3	5	83

## References

- Amiro, B. D., Todd, J. B., Wotton, B. M., Logan, K. A., Flannigan, M. D., Stocks, B. J., Mason, J. A., Martell, D. L. and Hirsch, K. G.: Direct carbon emissions from Canadian forest fires, 1959-1999, *Canadian Journal of Forest Research-Revue Canadienne De Recherche Forestière*, 31, 512–525, 2001.
- Bellassen, V., Le Maire, G., Dhôte, J. F., Ciais, P. and Viovy, N.: Modelling forest management within a global vegetation model--Part 1: Model structure and general behaviour, *Ecological Modelling*, 221(20), 2458–2474, doi:10.1016/j.ecolmodel.2010.07.008, 2010.
- Bond-Lamberty, B. and Gower, S. T.: Decomposition and Fragmentation of Coarse Woody Debris: Re-visiting a Boreal Black Spruce Chronosequence, *Ecosystems*, 11(6), 831–840, doi:10.1007/s10021-008-9163-y, 2008.
- Goulden, M., McMillan, A., Winston, G., Rocha, A., Manies, K., Harden, J. and Bond-Lamberty, B.: Patterns of NPP, GPP, respiration, and NEP during boreal forest succession, *GLOBAL CHANGE BIOLOGY*, 17(2), 855–871, doi:10.1111/j.1365-2486.2010.02274.x, 2011.
- Gower, S. T., Vogel, J. G., Norman, J. M., Kucharik, C. J., Steele, S. J. and Stow, T. K.: Carbon distribution and aboveground net primary production in aspen, jack pine, and black spruce stands in Saskatchewan and Manitoba, Canada, *J. Geophys. Res.*, 102(D24), 29029–29,041, doi:10.1029/97JD02317, 1997.
- De Groot, W. J., Pritchard, J. M. and Lynham, T. J.: Forest floor fuel consumption and carbon emissions in Canadian boreal forest fires, *Canadian Journal of Forest Research*, 39(2), 367–382, doi:10.1139/X08-192, 2009.
- Kane, E. S., Kasischke, E. S., Valentine, D. W., Turetsky, M. R. and McGuire, A. D.: Topographic influences on wildfire consumption of soil organic carbon in interior Alaska: Implications for black carbon accumulation, *Journal of Geophysical Research: Biogeosciences*, 112(G3), doi:10.1029/2007JG000458, 2007.
- Kasischke, E. S. and Hoy, E. E.: Controls on carbon consumption during Alaskan wildland fires, *Global Change Biology*, 18(2), 685–699, doi:10.1111/j.1365-2486.2011.02573.x, 2012.
- Kasischke, E. S., O'Neill K. P., French N. H. F. and Bourgeau-Chavez L. L.: Controls on patterns of biomass burning in Alaskan boreal forests, in: *Fire, Climate Change, and Carbon Cycling in the Boreal Forest*, edited by E. S. Kasischke and B. J. Stocks, pp. 173–196, Springer New York, 19-30, 2000.
- Manies, K. L. and Harden, J. W.: Soil data from different-age *Picea mariana* stands near Delta Junction, U.S. Department of the Interior, U.S. Geological Survey, Open-File Report 2011-1061, 4-5 pp., 2011.
- Manies, K. L., Harden, J. W., Bond-Lamberty, B. P. and O'Neill, K. P.: Woody debris along an upland chronosequence in boreal Manitoba and its impact on long-term carbon storage, *Canadian Journal of Forest Research*, 35(2), 472–482, doi:10.1139/x04-179, 2005.
- Manies, K. L., Harden, J. W., Silva, S. R., Briggs, P. H. and Schmid, B. M.: Soil Data from *Picea mariana* Stands near Delta Junction, Alaska of Different Ages and Soil Drainage Type, U.S. Department of the Interior, U.S. Geological Survey, Open-File Report 2004-1271, 4-5 pp., 2004.
- Manies, K. L., Harden, J. W. and Veldhuis, H.: Soil data from a moderately well and somewhat poorly drained fire chronosequence near Thompson, Manitoba, Canada. U.S., U.S.

Department of the Interior, U.S. Geological Survey, Open File Report 2006-1291, 4-5 pp., 2006.

- Newton, P. F.: Asymptotic size–density relationships within self-thinning black spruce and jack pine stand-types: Parameter estimation and model reformulations, *Forest Ecology and Management*, 226(1–3), 49–59, doi:10.1016/j.foreco.2006.01.023, 2006.
- Stocks, B. J.: Fire behavior in immature jack pine, *Canadian Journal of Forest Research*, 17(1): 80-86, 10.1139/x87-014, 1987.
- Stocks, B. J.: Fire behavior in mature jack pine, *Canadian Journal of Forest Research*, 19(6): 783-790, 10.1139/x89-119, 1989.
- Turetsky, M. R., Kane, E. S., Harden, J. W., Ottmar, R. D., Manies, K. L., Hoy, E. and Kasischke, E. S.: Recent acceleration of biomass burning and carbon losses in Alaskan forests and peatlands, *Nature Geoscience*, 4(1), 27–31, doi:10.1038/ngeo1027, 2011.
- Wang, C., Bond-Lamberty, B. and Gower, S.: Carbon distribution of a well-and poorly-drained black spruce fire chronosequence, *Global Change Biology*, 9(7), 1066–1079–1066–1079, 2003.
- Wang, T., Brender, P., Ciais, P., Piao, S., Mahecha, M. D., Chevallier, F., Reichstein, M., Ottlé, C., Maignan, F., Arain, A., Bohrer, G., Cescatti, A., Kiely, G., Law, B. E., Lutz, M., Montagnani, L., Moors, E., Osborne, B., Panferov, O., Papale, D. and Vaccari, F. P.: State-dependent errors in a land surface model across biomes inferred from eddy covariance observations on multiple timescales, *Ecological Modelling*, 246, 11–25, doi:10.1016/j.ecolmodel.2012.07.017, 2012.